Published in final edited form as:
J Cogn Neurosci. 2015 March ; 27(3): 464–473. doi:10.1162/jocn_a_00722.

Asymmetric Connectivity between the Anterior Temporal Lobe and the Language Network

Robert S. Hurley, **Borna Bonakdarpour**, **Xue Wang**, and **M. Marsel Mesulam**
Northwestern University, Chicago, IL

Abstract

The anterior temporal lobe (ATL) sits at the confluence of auditory, visual, olfactory, transmodal, and limbic processing hierarchies. In keeping with this anatomical heterogeneity, the ATL has been implicated in numerous functional domains, including language, semantic memory, social cognition, and facial identification. One question that has attracted considerable discussion is whether the ATL contains a mosaic of differentially specialized areas or whether it provides a domain-independent amodal hub. In the current study, based on task-free fMRI in right-handed neurologically intact participants, we found that the left lateral ATL is interconnected with hubs of the temporosylvian language network, including the inferior frontal gyrus and middle temporal gyrus of the ipsilateral hemisphere and, to a lesser extent, with homotopic areas of the contralateral hemisphere. In contrast, the right lateral ATL had much weaker functional connectivity with these regions in either hemisphere. Together with evidence that has been gathered in lesion-mapping and event-related neuroimaging studies, this asymmetry of functional connectivity supports the inclusion of the left ATL within the language network, a relationship that had been overlooked by classic aphasiology. The asymmetric domain selectivity for language of the left ATL, together with the absence of such an affiliation in the right ATL, is inconsistent with a strict definition of uniformly domain-independent amodal functionality in this region of the brain.

INTRODUCTION

The anterior temporal lobe (ATL) displays a high degree of architectonic and hodologic heterogeneity. In the monkey brain, it receives auditory pathways dorsally, visual pathways ventrally, and olfactory and limbic pathways medially. Transmodal cortex, located laterally in the ATL, provides a site for the integration of these afferent pathways (Moran, Mufson, & Mesulam, 1987). Indirect information on the connectivity of the human ATL has come from studies based on diffusion tensor imaging and resting state fMRI (Fan et al., 2013; Pascual et al., 2013; Binney, Parker, & Lambon Ralph, 2012). The former approach, based on the movement of water molecules in a magnetic field, delineates the heading of white matter tracts, whereas the latter approach, based on the interregional coherence of hemodynamic fluctuations, provides information that is potentially relevant to synaptic connectivity.

Reprint requests should be sent to: Dr. Robert S. Hurley, 320 E Superior St., Searle 11-579, Chicago, IL 60611, or via hurley@northwestern.edu.

The interregional hemodynamic coherence that underlies resting state functional connectivity (RSFC) is thought to reveal the presence of mono- or multisynaptic pathways. Support for this conjecture comes from observations of reduced RSFC after callosotomy (Johnston et al., 2008) and high correspondence of RSFC patterns with white matter pathways identified by diffusion tensor imaging (Honey et al., 2009; Skudlarski et al., 2008). This method has been applied to the exploration of ATL connectivity in the human brain. Pascual et al. (2013) recently demonstrated that the cytoarchitectonic subregions of ATL, as identified by Ding, Van Hoesen, Cassell, and Poremba (2009), have differential RSFC patterns in the human brain. The results of their analysis showed that, much like in the monkey brain (Moran et al., 1987), dorsal, ventral, and medial aspects of ATL were functionally connected with auditory, visual, and limbic cortices, respectively. Similar RSFC results were obtained by Fan et al. (2013) and linked to white matter pathways determined by diffusion tensor imaging.

The focus of this report is on the relationship of the ATL to the left hemisphere language network. ATL was omitted from the classic neurological model of language (Geschwind, 1965a, 1965b), probably because it is not vulnerable to isolated focal cerebrovascular accidents. Although observations on herpes simplex, temporal lobectomy, and intraoperative cortical stimulation had revealed language-related functions of the ATL (Damasio, 1992; Warrington & Shallice, 1984; Ojemann, 1983; Heilman, 1972), it took investigations on semantic dementia and primary progressive aphasia to fully reveal the profound importance of this region to language and aphasia (Mesulam et al., 2013; Hurley, Paller, Rogalski, & Mesulam, 2012; Patterson, Nestor, & Rogers, 2007; Jefferies & Lambon Ralph, 2006; Rogers et al., 2004; Hodges, Patterson, Oxbury, & Funnell, 1992; Snowden, Goulding, & Neary, 1989). This specialization of the ATL has received additional support from more recent observations based on neuroimaging with PET, fMRI, magnetoencephalography, and electrocorticography, voxel-based lesion mapping in patients with focal neural injury, and computational modeling (Abel et al., 2014; Ueno, Saito, Rogers, & Lambon Ralph, 2011; Visser, Jefferies, & Lambon Ralph, 2010; Schwartz et al., 2009; Taylor, Stamatakis, & Tyler, 2009; Gitelman, Nobre, Sonty, Parrish, & Mesulam, 2005; Damasio, Tranel, Grabowski, Adolphs, & Damasio, 2004; Marinkovic et al., 2003). Furthermore, “virtual lesions” in lateral left ATL caused by TMS have been shown to impair verbal semantic judgments (Campanella, Fabbro, & Urgesi, 2013; Lambon Ralph, Pobric, & Jefferies, 2009; Pobric, Jefferies, & Ralph, 2007).

Considerable attention has been directed to the type of language function associated with the left ATL. Left ATL has been shown to be involved in the labeling of unique concrete entities, both for visual objects such as faces and landmarks (Tranel, 2006; Grabowski et al., 2001; Damasio, Grabowski, Tranel, Hichwa, & Damasio, 1996) and for auditory objects such as musical passages and famous voices (Belfi & Tranel, 2014; Waldron, Manzel, & Tranel, 2014; Grabowski et al., 2001; Damasio et al., 1996). The left ATL also seems to play a critical role in odor naming (Olofsson, Hurley, Bowman, Mesulam, & Gottfried, submitted; Gefen et al., 2013; Olofsson, Rogalski, Harrison, Mesulam, & Gottfried, 2013). In picture–word verification tasks, primary progressive aphasia patients with left ATL lesions perform poorly when asked to differentiate words from the same object category (e.g., “cat” vs. “dog”), but performance becomes nearly normal when the patients are asked

to differentiate words that denote objects of different categories (e.g., “cat” vs. “hammer”). This taxonomic interference effect is not seen in similarly modeled tasks that probe nonverbal associations of objects (Hurley et al., 2012). On the basis of such findings, we have proposed that processing in left ATL helps to establish fine-grain specificity in word meaning, allowing for precise mapping between linguistic and object representations (Mesulam et al., 2013).

The hodological foundations of the language-related asymmetric functionality of the ATL are poorly understood. Some have used seed-based RSFC approaches to study ATL connectivity, where hemodynamic activity is measured in a predetermined ROI known as a “seed,” and then correlated with the time courses of all other voxels in the brain. Some of these investigations have focused exclusively on the connectivity of ATL seeds in the left hemisphere (Pascual et al., 2013; Warren, Crinion, Lambon Ralph, & Wise, 2009). Others have seeded both hemispheres but have not conducted quantitative comparisons of resultant RSFC maps from left versus right hemispheric seeds (Fan et al., 2013; Guo et al., 2013).

In the current study, we used a seed-based approach to investigate the intrahemispheric and interhemispheric RSFC of the ATL and two other key language regions: the posterior middle temporal gyrus (MTG) and the pars triangularis of the inferior frontal gyrus (IFG). The pars triangularis of the IFG was chosen as one of the seed areas, because it is a component of Broca’s area, a region that has been included as a major epicenter of the classic language network for more than 150 years (Broca, 1861), and is among the most consistently activated regions in neuroimaging studies of language (Indefrey & Levelt, 2004). The posterior MTG was chosen as another seed region, because lesion mapping studies have shown that many of the lexicosemantic functions originally ascribed to Wernicke’s area can be linked to the integrity of this part of the temporal lobe (Baldo, Arevalo, Patterson, & Dronkers, 2013; Ogar et al., 2011; Turken & Dronkers, 2011; Dronkers, Wilkins, Van Valin, Redfern, & Jaeger, 2004). It has been shown that MTG and IFG jointly contribute to semantic processing (Jefferies, 2013; Gow, 2012; Hagoort, 2005), that they are more strongly interconnected during language tasks (Snijders, Petersson, & Hagoort, 2010), and that TMS in either region disrupts verbal processing (Acheson & Hagoort, 2013; Whitney, Kirk, O’Sullivan, Lambon Ralph, & Jefferies, 2012).

Seeds were placed in ATL, IFG, and MTG in both hemispheres to quantitatively compare RSFC maps from homotopic regions of the left and right hemispheres. We analyzed RSFC patterns to confirm that the two nodes of the traditional language network, MTG and IFG, are more strongly interconnected in the left than right hemisphere as suggested by previous RSFC investigations (Gotts et al., 2013; Nielsen, Zielinski, Ferguson, Lainhart, & Anderson, 2013; Liu, Stufflebeam, Sepulcre, Hedden, & Buckner, 2009). Our second goal was to determine whether ATL demonstrates a similar asymmetry of connectivity. The confirmation of such asymmetry would further support the inclusion of the left ATL into the language network and would show that the ATL of each hemisphere displays regional domain specificity rather than uniformly amodal functionality.

METHODS

Participants

Thirty-three right-handed, native English-speaking neurologically unimpaired adults (15 men) took place in the study. They were recruited to serve as normal controls for an ongoing longitudinal study of primary progressive aphasia. Mean age was 63.5 ± 7.0 (*SD*) years.

Image Acquisition

MR images were acquired with a Siemens Trio 3-T scanner. All participants were scanned for 10 min and were instructed to stay awake with eyes open. Images were collected using a gradient-echo T2-weighted sequence (repetition time = 2500 msec, echo time = 20 msec, flip angle = 80°, field of view = 220, 3 × 3 × 3 mm voxel size). Structural MR images were also collected using a T1-weighted 3-D MPRAGE sequence (repetition time = 2300 msec, echo time = 2.91 msec, flip angle = 9°, field of view = 256, 1 × 1 × 1 mm voxel size).

Preprocessing

SPM8 (www.fil.ion.ucl.ac.uk/spm/) was used for image processing and analysis. The DPARSF toolbox was used to preprocess functional images (Chao-Gan & Yu-Feng, 2010). After slice timing correction and realignment, functional images were coregistered to the structural images and transformed into MNI standard space (Montreal Neurological Institute) using the DARTEL algorithm (Ashburner, 2007). The images were then smoothed using a 66-mm FWHM Gaussian kernel, detrended, and bandpass filtered from 0.01 to 0.08 Hz. Images with greater than 1 mm scan-to-scan movement (2.4 ± 3.7, mean ± *SD*, out of the 244 total volumes) were interpolated using the ArtRepair Toolbox (Mazaika, Hoeft, Glover, & Reiss, 2009). Nuisance variables were then regressed out of each hemodynamic time course, including affine motion parameters, the global mean signal, white matter signal, and cerebrospinal fluid signal.

Defining ROIs

Ten-millimeter spherical ROIs were constructed in candidate language regions in each hemisphere in normalized MNI space. The pars triangularis of the IFG ($x = \pm54$, $y = 24$, $z = 3$) was identified on the basis of its anatomical landmarks. The posterior MTG location ($x = \pm66$, $y = -38$, $z = -4$) coincided with the area of lexicosemantic functionality identified by Turken and Dronkers (2011). The ATL seed ($x = \pm50$, $y = 11$, $z = -32$) was placed in a lateral portion of ATL, just past the anterior limit of MTG. This location overlaps with peak atrophy sites in patients with word comprehension impairments as well as the functional activation sites associated with synonym identification tasks (Mesulam et al., 2013; Gitelman et al., 2005). In the left hemisphere, this lateral portion of ATL has also been shown to have ipsilateral RSFC connections with other language regions (Pascual et al., 2013; Warren et al., 2009). To determine if asymmetry was specific to the language network, two nodes of the spatial attention network known to have functional interconnections (Van Dijk et al., 2010) were chosen as control sites and explored in both hemispheres with 4-mm spherical ROIs placed in the intraparietal sulci ($x = \pm23$, $y = -58$, $z = 53$) and FEFs ($x = \pm26$, $y = -5$, $z = 58$).

Generation of Whole-brain Functional Connectivity Maps

Seed-based RSFC maps were created using the REST toolkit (Song et al., 2011). The hemodynamic time series from all voxels included in the ROI seed were averaged and correlated with the individual time series from all other voxels in the brain. The Pearson correlation coefficients were then stabilized with Fischer's *Z* transformation. It is common in resting state analysis to average the individual *z*(*r*) maps and threshold the group *z*(*r*) map with a liberal criteria (e.g., $z > .04$; Pascual et al., 2013; Van Dijk et al., 2010). In this study, we wanted to more easily visualize selective connections between seeds and other cognitive hubs, so employed a more stringent-than-usual criteria for thresholding. The individual *Z* values were used to create group one-sample *t* maps, revealing areas that were functionally connected to each seed, and those *t* maps were thresholded using a false discovery rate (FDR) of $p < .001$ (Genovese, Lazar, & Nichols, 2002).

Hemodynamic Correlations between ROI Seeds

Correlations were computed between the averaged time series of ROIs. Each of the three possible correlations between pairs of ipsilateral ROIs was examined separately in the left hemisphere and the right hemisphere. The Pearson coefficients were *Z*-transformed and averaged across participants. One-sample *t* tests were used to examine whether each correlation was significantly different from zero. Paired *t* tests were used to compare the magnitude of left versus right hemispheric correlations. This same procedure was also used to compare the magnitude of correlations between the two spatial attention control sites in each hemisphere.

Voxel Counts in Each ROI

In each seed-based connectivity map (IFG, MTG, and ATL in each hemisphere), the number of significantly correlated 3-mm voxels falling in the boundaries of the other two ipsilateral ROI "targets" were counted. The SPM gray matter probability template was used to exclude any nongray matter voxels within the target ROIs from analysis. Ratios were computed between the number of seed-correlated voxels over the total number of gray matter voxels (104 ± 10.2, mean ± *SD*) in each ROI.

RESULTS

Whole-brain Seed-based Connectivity Mapping

ATL is often subject to distortion and signal dropout in fMRI, which may result in failure to detect ATL activations with event-related designs (Visser et al., 2010). In the current study, the temporal signal-to-noise ratios in each of the seed ROIs were =58, indicating adequate signal was obtained for analysis (Marcus et al., 2013). RSFC maps were created by correlating the averaged hemodynamic time series from the voxels in each seed with the individual time series from all other voxels in the brain. Each *t* map was thresholded using an FDR of $p < .001$, using the critical *t* value as the lowerbounds for flamescale plots and doubling that value for the upperbounds. Negative *t* values were not plotted, as anticorrelations are difficult to interpret in rs-fMRI (Murphy, Birn, Handwerker, Jones, & Bandettini, 2009) and are not relevant to our hypotheses. Employing these stringent

thresholds, all seed regions showed regionally delineated and anatomically distinct connectivity patterns. All seed areas had a halo of strong local connections as well as connections with the homotopic area in the contralateral hemisphere (Figures 1–3, 5).

When comparing connectivity of left and right hemispheric seeds, asymmetries in RSFC emerged. Left-hemispheric seeds in commonly accepted centers of the language network: IFG and MTG showed extensive ipsilateral connectivity with a widespread network of noncontiguous structures (Figures 1 and 2A). This network includes the seed regions (IFG, MTG, and ATL), the angular gyrus, and frontal structures including premotor cortex and the superior frontal gyrus. Contralateral connections with right hemispheric structures tended to be relatively constrained or altogether absent. Informatively, right-hemispheric seeds in IFG and MTG were only sparsely connected with this network of regions (Figures 1 and 2B) in both the ipsilateral and contralateral hemispheres. The angular gyrus shows a possible exception to this pattern, as it appears to share ipsilateral connections with IFG and MTG in both hemispheres (Figures 1 and 2A, B).

Surprisingly, lateral ATL displayed the most conspicuous asymmetry of all seed regions investigated (Figure 3). Left ATL demonstrated ipsilateral connections with the same network of regions identified in the IFG and MTG-based maps (Figure 3A), with the exception that no connectivity was observed with premotor cortex. In contrast, right ATL appears to show much less ipsilateral and contralateral connectivity with IFG, the angular gyrus, and the superior frontal gyrus (Figure 3B). In summary, lateral ATL shows an RSFC pattern quite similar to other commonly accepted epicenters of the language network.

RSFC maps from IFG, MTG, and ATL in the left hemisphere appear to largely overlap across a wide network of ipsilateral regions. RSFC maps from homotopic seeds in the right hemisphere tended to be more closely constrained to the halo immediately surrounding the seed region, therefore showing considerably less overlap in their mappings. To more easily visualize these hemispheric differences, those voxels that were significant in all three left-hemispheric and/or right-hemispheric seed-based maps are plotted in Figure 4. The overlapping RSFC of left hemispheric seeds (in red) suggests their common participation in a large-scale functional network in the left hemisphere, including the seed regions plus the superior frontal gyrus and angular gyrus. In contrast, right-hemispheric seeds shared only minimal overlap in a small section of right MTG.

The possibility that these asymmetries of connectivity in the language network were nonspecific or spurious was explored by examining RSFC maps from nodes in another large-scale distributed network, namely the frontoparietal network that underlies the distribution of spatial attention. We hypothesized that the intraparietal sulci and FEFs would show relatively symmetric RSFC patterns. RSFC maps from seeds in both left and right intraparietal sulci (Figure 5) appear to fulfill this expectation. Both seeds were connected with a wide swath of adjacent parietal cortex and showed longer-range connections with frontal components of the spatial attention network including the FEFs. This network is markedly symmetric: Ipsilateral RSFC patterns are quite similar to contralateral patterns, and maps are similar for both left-hemispheric and right-hemispheric seeds.

Inter-ROI Correlational Analyses

Left-hemispheric nodes of the language network appeared to share reciprocal interconnections, such that IFG is ipsilaterally connected with MTG and ATL and vice versa (Figures 1–3A, 4). In contrast, interconnections between homotopic regions in the right hemisphere appear tenuous to nonexistent (Figures 1–3B, 4). We wanted to more rigorously quantify these patterns and to directly contrast the degree of interconnectedness between ipsilateral nodes in each hemisphere. Contralateral connections were not examined in these ROI analyses. Two types of inter-ROI correlational analyses were performed: an assessment of average strength of correlation and an assessment of the spatial extent of correlated voxels. The strength of RSFC between pairs of ipsilateral ROIs was quantitated by correlating their extracted time series, averaged across all voxels in each ROI (Figure 6A). One-sample *t* tests revealed that all intrahemispheric ROI correlations were significantly greater than zero, in both hemispheres ($p < .005$ for all tests; Table 1). Paired *t* tests revealed, however, that the three correlation coefficients (IFG–ATL, IFG–MTG, MTG–ATL) in the left hemisphere were all of higher magnitude than their counterparts in the right hemisphere ($p < .01$ for all tests; Figure 6A, Table 1).

Interconnections between the two hubs of the spatial attention network, the intraparietal sulcus and FEF, were found to be significant in both hemispheres (Table 1). Unlike language regions, however, connectivity strength did not differ by hemisphere, indicating that the asymmetries in Figures 1–4 reflect a specific property of the language network rather than a general feature of all large-scale functional networks.

The spatial extent of correlated activity between ipsilateral ROIs was also examined. In each seed-based RSFC map (Figures 1–3), the number of significantly correlated voxels falling in the boundaries of the other two ipsilateral ROI “targets” were counted. The proportion of target gray matter voxels in each ROI that are functionally connected with the seed region are shown in Figure 6B. In all cases, a much larger proportion of the target voxels were functionally connected with seeds in the left hemisphere. The most prominent asymmetry was shown by the ATL where the percentage of significantly interconnected voxels ranged from 18% to 77% in the left hemisphere and from 0 to 6% in the right.

DISCUSSION

Our RSFC results are consistent with existing accounts of the left hemisphere language network. Whole-brain mapping showed that IFG, MTG, and ATL left-hemispheric seeds displayed reciprocal interconnections and were also connected with the left angular gyrus and superior frontal gyrus. In totality, this set of regions is in close alignment with the currently accepted components of the language network (Jefferies, 2013; Price, 2012; Binder, Desai, Graves, & Conant, 2009). In addition, IFG and MTG showed connectivity with left premotor cortex (Figures 1 and 2A), which is involved in speech production (Krieger-Redwood, Gaskell, Lindsay, & Jefferies, 2013; Okada & Hickok, 2006). The ATL failed to show such a premotor connection, fitting with the notion that ATL is more heavily involved in language comprehension than production (Rogalski et al., 2011).

Lateralization of function is the most distinct feature of the human brain and is most conspicuous in the organization of language (Knecht et al., 2000; Borod, Carper, Naeser, & Goodglass, 1985). The within-subject experimental design of this study allowed a rigorous comparison of RSFC from seeds in the left and right hemispheres, so that the asymmetry of connectivity could be established quantitatively. In keeping with left hemispheric dominance for language, the connectivity of IFG, MTG, and ATL seeds in the left hemisphere was more extensive than that of homotopic right hemispheric seeds. This asymmetry was particularly striking in the ATL. Whole-brain seed mapping showed that the left ATL was strongly interconnected not only with the IFG, MTG, angular gyrus, and superior frontal gyrus in the ipsilateral left hemisphere but also, albeit to a lesser extent, with these areas in the contralateral right hemisphere (Figure 3A). In contrast, whole-brain mapping from right ATL failed to show prominent connections with IFG, the angular gyrus, or superior frontal gyrus in either hemisphere (Figure 3B). In addition, inter-ROI time course correlations and voxel counts (Figure 6) showed that ipsilateral connectivity of the right ATL seed with IFG and MTG was much less extensive than shown by the left ATL seed.

The possibility that this asymmetry could represent a general feature of the left hemisphere rather than a special property of the language network was addressed by carrying out a similar analysis of RSFC in the two epicenters of the frontoparietal spatial attention network, the intraparietal sulci, and FEFs (Mesulam, 1999). The interconnectivity between these two areas did not display hemispheric asymmetry, showing that the left lateralization of the interconnections among IFG, MTG, and ATL is a distinctive property of the language network.

The greater physiological coupling between left temporosylvian language regions shown in Figure 6 may reflect hemispheric differences in the structure of their white matter interconnections (Parker et al., 2005). For example, the direct component of the arcuate fasciculus, which connects inferior frontal with posterior temporal regions, is more prominent in the left hemisphere in most individuals (Catani et al., 2007). Whether such asymmetry exists in the fiber pathways that connect ATL with other components of the language network (especially the IFG) remains to be determined, although the presence of asymmetric leftward fractional anisotropy in the uncinate and middle longitudinal fasciculus suggests this is a likely scenario (Menjot de Champfleur et al., 2013; Powell et al., 2012; Hasan et al., 2009).

The RSFC connections of left ATL were strikingly similar to those shown by IFG and MTG, both commonly accepted hubs of the language network. The current results together with a growing literature based on functional neuroimaging and the investigation of patients with neurological diseases further strengthen the conclusion that the ATL in the left hemisphere is specialized for language, especially for fine-grained verbal representations that underlie word comprehension and object naming. The most convincing demonstration of this relationship comes from primary progressive aphasia patients with peak atrophy sites confined to the left ATL (Mesulam et al., 2013). Such patients show severe comprehension and naming impairments in the absence of equivalent impairments in processing nonverbal associations of objects, at least in tasks where objects are presented visually. In contrast, there are no documented cases of aphasia caused by right unilateral ATL lesions (Lambon

Ralph, Cipolotti, Manes, & Patterson, 2010), unless such individuals also happen to be right-hemispheric dominant for language (Drane et al., 2009). The right ATL does not therefore appear to play a critical role in language processing. This is not to say that the left ATL is exclusively dedicated to language or that the right ATL makes no contribution to language, but that each ATL has distinctly different sets of functions for which it plays a critical rather than participatory role. This arrangement, characteristic of all other transmodal areas of the human brain, is somewhat inconsistent with the "strong" version of the semantic hub account (Patterson et al., 2007), which appears to attribute a domain-independent and amodal functionality to both ATLs, leading to the expectation that ATL damage on either side should cause impairments of semantic memory distributed across all modalities and domains.

A more recent version of the semantic hub account recognizes the presence of hemispheric asymmetry in the functionality of ATL (Lambon Ralph, 2014; Schapiro, McClelland, Welbourne, Rogers, & Lambon Ralph, 2013; Binney et al., 2012; Visser & Lambon Ralph, 2011). According to this "graded connectivity" version, truly global semantic impairments should arise only after bilateral ATL lesions, an inference that is consistent with the hemispheric specialization patterns revealed by our RSFC results. In keeping with this version of ATL functionality, impairment in naming (but not recognizing) famous faces was correlated with atrophy in the left ATL whereas the more global impairment in both naming and recognizing the depicted person was correlated with ATL atrophy in both hemispheres (Gefen et al., 2013). It appears, therefore, that neither the left nor right ATL is, by itself, strictly amodal. Collectively, however, the left and right ATLs encompass neural resources that mediate a large array of transmodal associations, including many verbal, nonverbal, and experiential components of semantic memory.

In conclusion, the present findings provide a plausible physiologic account of left hemispheric dominance for language, and show that the left lateral ATL has a profoundly asymmetric connectivity that embeds it within the language network. The anterior temporal cortex is one of the most complex of all transmodal regions in the human brain. Future studies will help to delineate the mosaic of domain-selective and asymmetric specializations of this area.

Acknowledgments

This work was supported by the National Institute on Deafness and Other Communication Disorders (R01 DC008552). Additional support for R. S. H. was provided by the National Institute on Aging Mechanisms of Aging and Dementia Training Grant (NIA T32 AG20506). The authors thank Todd Parrish for designing the MRI sequences, Adam Martersteck for acquiring the MRI scans, and Christina Wieneke for coordinating participant assessments.

References

Abel TJ, Rhone AE, Nourski KV, Granner MA, Oya H, Griffiths TD, et al. Mapping the temporal pole with a specialized electrode array: Technique and preliminary results. Physiological Measurement. 2014; 35:323–337. [PubMed: 24480831]

Acheson DJ, Hagoort P. Stimulating the brain's language network: Syntactic ambiguity resolution after TMS to the inferior frontal gyrus and middle temporal gyrus. Journal of Cognitive Neuroscience. 2013; 25:1664–1677. [PubMed: 23767923]

Ashburner J. A fast diffeomorphic image registration algorithm. Neuroimage. 2007; 38:95–113. [PubMed: 17761438]

Baldo JV, Arevalo A, Patterson JP, Dronkers NF. Grey and white matter correlates of picture naming: Evidence from a voxel-based lesion analysis of the Boston Naming Test. Cortex. 2013; 49:658–667. [PubMed: 22482693]

Belfi AM, Tranel D. Impaired naming of famous musical melodies is associated with left temporal polar damage. Neuropsychology. 2014; 28:429–435. [PubMed: 24364392]

Binder JR, Desai RH, Graves WW, Conant LL. Where is the semantic system? A critical review and meta-analysis of 120 functional neuroimaging studies. Cerebral Cortex. 2009; 19:2767–2796. [PubMed: 19329570]

Binney RJ, Parker GJ, Lambon Ralph MA. Convergent connectivity and graded specialization in the rostral human temporal lobe as revealed by diffusion-weighted imaging probabilistic tractography. Journal of Cognitive Neuroscience. 2012; 24:1998–2014. [PubMed: 22721379]

Borod JC, Carper M, Naeser M, Goodglass H. Left-handed and right-handed aphasics with left hemisphere lesions compared on nonverbal performance measures. Cortex. 1985; 21:81–90. [PubMed: 3987313]

Broca, P. Sur siege de la faculte du langage articule avec deux observations d'aphemie (perte de la parole). Paris: Victor Masson et Fils; 1861.

Campanella F, Fabbro F, Urgesi C. Cognitive and anatomical underpinnings of the conceptual knowledge for common objects and familiar people: A repetitive transcranial magnetic stimulation study. PLoS One. 2013; 8:e64596. [PubMed: 23704999]

Catani M, Allin MP, Husain M, Pugliese L, Mesulam MM, Murray RM, et al. Symmetries in human brain language pathways correlate with verbal recall. Proceedings of the National Academy of Sciences, USA. 2007; 104:17163–17168.

Chao-Gan Y, Yu-Feng Z. DPARSF: A MATLAB toolbox for "pipeline" data analysis of resting-state fMRI. Frontiers in Systems Neuroscience. 2010; 4:13. [PubMed: 20577591]

Damasio AR. Aphasia. New England Journal of Medicine. 1992; 326:531–539. [PubMed: 1732792]

Damasio H, Grabowski TJ, Tranel D, Hichwa RD, Damasio AR. A neural basis for lexical retrieval. Nature. 1996; 380:499–505. [PubMed: 8606767]

Damasio H, Tranel D, Grabowski T, Adolphs R, Damasio A. Neural systems behind word and concept retrieval. Cognition. 2004; 92:179–229. [PubMed: 15037130]

Ding SL, Van Hoesen GW, Cassell MD, Poremba A. Parcellation of human temporal polar cortex: A combined analysis of multiple cytoarchitectonic, chemoarchitectonic, and pathological markers. Journal of Comparative Neurology. 2009; 514:595–623. [PubMed: 19363802]

Drane DL, Ojemann GA, Ojemann JG, Aylward E, Silbergeld DL, Miller JW, et al. Category-specific recognition and naming deficits following resection of a right anterior temporal lobe tumor in a patient with atypical language lateralization. Cortex. 2009; 45:630–640. [PubMed: 18632095]

Dronkers NF, Wilkins DP, Van Valin RD Jr, Redfern BB, Jaeger JJ. Lesion analysis of the brain areas involved in language comprehension. Cognition. 2004; 92:145–177. [PubMed: 15037129]

Fan L, Wang J, Zhang Y, Han W, Yu C, Jiang T. Connectivity-based parcellation of the human temporal pole using diffusion tensor imaging. Cerebral Cortex. 2013

Gefen T, Wieneke C, Martersteck A, Whitney K, Weintraub S, Mesulam MM, et al. Naming vs knowing faces in primary progressive aphasia: A tale of 2 hemispheres. Neurology. 2013; 81:658–664. [PubMed: 23940020]

Genovese CR, Lazar NA, Nichols T. Thresholding of statistical maps in functional neuroimaging using the false discovery rate. Neuroimage. 2002; 15:870–878. [PubMed: 11906227]

Gitelman DR, Nobre AC, Sonty S, Parrish TB, Mesulam MM. Language network specializations: An analysis with parallel task designs and functional magnetic resonance imaging. Neuroimage. 2005; 26:975–985. [PubMed: 15893473]

Gotts SJ, Jo HJ, Wallace GL, Saad ZS, Cox RW, Martin A. Two distinct forms of functional lateralization in the human brain. Proceedings of the National Academy of Sciences, USA. 2013; 110:E3435–E3444.

Gow DW Jr. The cortical organization of lexical knowledge: A dual lexicon model of spoken language processing. Brain and Language. 2012; 121:273–288. [PubMed: 22498237]

Grabowski TJ, Damasio H, Tranel D, Ponto LL, Hichwa RD, Damasio AR. A role for left temporal pole in the retrieval of words for unique entities. Human Brain Mapping. 2001; 13:199–212. [PubMed: 11410949]

Guo CC, Gorno-Tempini ML, Gesierich B, Henry M, Trujillo A, Shany-Ur T, et al. Anterior temporal lobe degeneration produces widespread network-driven dysfunction. Brain. 2013; 136:2979–2991. [PubMed: 24072486]

Hagoort P. On Broca, brain, and binding: A new framework. Trends in Cognitive Sciences. 2005; 9:416–423. [PubMed: 16054419]

Hasan KM, Iftikhar A, Kamali A, Kramer LA, Ashtari M, Cirino PT, et al. Development and aging of the healthy human brain uncinate fasciculus across the lifespan using diffusion tensor tractography. Brain Research. 2009; 1276:67–76. [PubMed: 19393229]

Heilman KM. Anomic aphasia following anterior temporal lobectomy. Transactions of the American Neurological Association. 1972; 97:291–293.

Hodges JR, Patterson K, Oxbury S, Funnell E. Semantic dementia. Progressive fluent aphasia with temporal lobe atrophy. Brain. 1992; 115:1783–1806. [PubMed: 1486461]

Honey CJ, Sporns O, Cammoun L, Gigandet X, Thiran JP, Meuli R, et al. Predicting human resting-state functional connectivity from structural connectivity. Proceedings of the National Academy of Sciences, USA. 2009; 106:2035–2040.

Hurley RS, Paller KA, Rogalski EJ, Mesulam MM. Neural mechanisms of object naming and word comprehension in primary progressive aphasia. Journal of Neuroscience. 2012; 32:4848–4855. [PubMed: 22492040]

Indefrey P, Levelt WJ. The spatial and temporal signatures of word production components. Cognition. 2004; 92:101–144. [PubMed: 15037128]

Jefferies E. The neural basis of semantic cognition: Converging evidence from neuropsychology, neuroimaging and TMS. Cortex. 2013; 49:611–625. [PubMed: 23260615]

Jefferies E, Lambon Ralph MA. Semantic impairment in stroke aphasia versus semantic dementia: A case-series comparison. Brain. 2006; 129:2132–2147. [PubMed: 16815878]

Johnston JM, Vaishnavi SN, Smyth MD, Zhang D, He BJ, Zempel JM, et al. Loss of resting interhemispheric functional connectivity after complete section of the corpus callosum. Journal of Neuroscience. 2008; 28:6453–6458. [PubMed: 18562616]

Knecht S, Drager B, Deppe M, Bobe L, Lohmann H, Floel A, et al. Handedness and hemispheric language dominance in healthy humans. Brain. 2000; 123:2512–2518. [PubMed: 11099452]

Krieger-Redwood K, Gaskell MG, Lindsay S, Jefferies E. The selective role of premotor cortex in speech perception: A contribution to phoneme judgements but not speech comprehension. Journal of Cognitive Neuroscience. 2013; 25:2179–2188. [PubMed: 23937689]

Lambon Ralph MA. Neurocognitive insights on conceptual knowledge and its breakdown. Philosophical Transactions of the Royal Society of London, Series B, Biological Sciences. 2014; 369:20120392.

Lambon Ralph MA, Cipolotti L, Manes F, Patterson K. Taking both sides: Do unilateral anterior temporal lobe lesions disrupt semantic memory? Brain. 2010; 133:3243–3255. [PubMed: 20952378]

Lambon Ralph MA, Pobric G, Jefferies E. Conceptual knowledge is underpinned by the temporal pole bilaterally: Convergent evidence from rTMS. Cerebral Cortex. 2009; 19:832–838. [PubMed: 18678765]

Liu H, Stufflebeam SM, Sepulcre J, Hedden T, Buckner RL. Evidence from intrinsic activity that asymmetry of the human brain is controlled by multiple factors. Proceedings of the National Academy of Sciences, USA. 2009; 106:20499–20503.

Marcus DS, Harms MP, Snyder AZ, Jenkinson M, Wilson JA, Glasser MF, et al. Human Connectome Project informatics: Quality control, database services, and data visualization. Neuroimage. 2013; 80:202–219. [PubMed: 23707591]

Marinkovic K, Dhond RP, Dale AM, Glessner M, Carr V, Halgren E. Spatiotemporal dynamics of modality-specific and supramodal word processing. Neuron. 2003; 38:487–497. [PubMed: 12741994]

Mazaika, P.; Hoeft, F.; Glover, GH.; Reiss, AL. Methods and software for fMRI analysis for clinical subjects. Paper presented at the Organization for Human Brain Mapping Conference; 2009.

Menjot de Champfleur N, Lima Maldonado I, Moritz-Gasser S, Machi P, Le Bars E, Bonafe A, et al. Middle longitudinal fasciculus delineation within language pathways: A diffusion tensor imaging study in human. European Journal of Radiology. 2013; 82:151–157. [PubMed: 23084876]

Mesulam MM. Spatial attention and neglect: Parietal, frontal and cingulate contributions to the mental representation and attentional targeting of salient extrapersonal events. Philosophical Transactions of the Royal Society of London, Series B, Biological Sciences. 1999; 354:1325–1346.

Mesulam MM, Wieneke C, Hurley R, Rademaker A, Thompson CK, Weintraub S, et al. Words and objects at the tip of the left temporal lobe in primary progressive aphasia. Brain. 2013; 136:601–618. [PubMed: 23361063]

Moran MA, Mufson EJ, Mesulam MM. Neural inputs into the temporopolar cortex of the rhesus monkey. Journal of Comparative Neurology. 1987; 256:88–103. [PubMed: 3819040]

Murphy K, Birn RM, Handwerker DA, Jones TB, Bandettini PA. The impact of global signal regression on resting state correlations: Are anti-correlated networks introduced? Neuroimage. 2009; 44:893–905. [PubMed: 18976716]

Nielsen JA, Zielinski BA, Ferguson MA, Lainhart JE, Anderson JS. An evaluation of the left-brain vs. right-brain hypothesis with resting state functional connectivity magnetic resonance imaging. PLoS One. 2013; 8:e71275. [PubMed: 23967180]

Ogar JM, Baldo JV, Wilson SM, Brambati SM, Miller BL, Dronkers NF, et al. Semantic dementia and persisting Wernicke's aphasia: Linguistic and anatomical profiles. Brain and Language. 2011; 117:28–33. [PubMed: 21315437]

Ojemann GA. Brain organization for language from the perspective of electrical stimulation. Behavioral and Brain Science. 1983; 6:189–230.

Okada K, Hickok G. Left posterior auditory-related cortices participate both in speech perception and speech production: Neural overlap revealed by fMRI. Brain and Language. 2006; 98:112–117. [PubMed: 16716388]

Olofsson JK, Hurley RS, Bowman NE, Mesulam MM, Gottfried JA. A designated odor-language integration system in the human brain. submitted.

Olofsson JK, Rogalski E, Harrison T, Mesulam MM, Gottfried JA. A cortical pathway to olfactory naming: Evidence from primary progressive aphasia. Brain. 2013; 136:1245–1259. [PubMed: 23471695]

Parker GJ, Luzzi S, Alexander DC, Wheeler-Kingshott CA, Ciccarelli O, Lambon Ralph MA. Lateralization of ventral and dorsal auditory-language pathways in the human brain. Neuroimage. 2005; 24:656–666. [PubMed: 15652301]

Pascual B, Masdeu JC, Hollenbeck M, Makris N, Insausti R, Ding SL, et al. Large-scale brain networks of the human left temporal pole: A functional connectivity MRI study. Cerebral Cortex. 2013

Patterson K, Nestor PJ, Rogers TT. Where do you know what you know? The representation of semantic knowledge in the human brain. Nature Reviews Neuroscience. 2007; 8:976–987.

Pobric G, Jefferies E, Ralph MA. Anterior temporal lobes mediate semantic representation: Mimicking semantic dementia by using rTMS in normal participants. Proceedings of the National Academy of Sciences, USA. 2007; 104:20137–20141.

Powell JL, Parkes L, Kemp GJ, Sluming V, Barrick TR, Garcia-Finana M. The effect of sex and handedness on white matter anisotropy: A diffusion tensor magnetic resonance imaging study. Neuroscience. 2012; 207:227–242. [PubMed: 22274289]

Price CJ. A review and synthesis of the first 20 years of PET and fMRI studies of heard speech, spoken language and reading. Neuroimage. 2012; 62:816–847. [PubMed: 22584224]

Rogalski E, Cobia D, Harrison TM, Wieneke C, Thompson CK, Weintraub S, et al. Anatomy of language impairments in primary progressive aphasia. The Journal of Neuroscience: The Official Journal of the Society for Neuroscience. 2011; 31:3344–3350. [PubMed: 21368046]

Rogers TT, Lambon Ralph MA, Garrard P, Bozeat S, McClelland JL, Hodges JR, et al. Structure and deterioration of semantic memory: A neuropsychological and computational investigation. Psychological Review. 2004; 111:205–235. [PubMed: 14756594]

Schapiro AC, McClelland JL, Welbourne SR, Rogers TT, Lambon Ralph MA. Why bilateral damage is worse than unilateral damage to the brain. Journal of Cognitive Neuroscience. 2013; 25:2107–2123. [PubMed: 23806177]

Schwartz MF, Kimberg DY, Walker GM, Faseyitan O, Brecher A, Dell GS, et al. Anterior temporal involvement in semantic word retrieval: Voxel-based lesion-symptom mapping evidence from aphasia. Brain. 2009; 132:3411–3427. [PubMed: 19942676]

Skudlarski P, Jagannathan K, Calhoun VD, Hampson M, Skudlarska BA, Pearlson G. Measuring brain connectivity: Diffusion tensor imaging validates resting state temporal correlations. Neuroimage. 2008; 43:554–561. [PubMed: 18771736]

Snijders TM, Petersson KM, Hagoort P. Effective connectivity of cortical and subcortical regions during unification of sentence structure. Neuroimage. 2010; 52:1633–1644. [PubMed: 20493954]

Snowden JS, Goulding PJ, Neary D. Semantic dementia: A form of circumscribed cerebral atrophy. Behavioural Neurology. 1989; 2:167–182.

Song XW, Dong ZY, Long XY, Li SF, Zuo XN, Zhu CZ, et al. REST: A toolkit for resting-state functional magnetic resonance imaging data processing. PLoS One. 2011; 6:e25031. [PubMed: 21949842]

Taylor KI, Stamatakis EA, Tyler LK. Crossmodal integration of object features: Voxel-based correlations in brain-damaged patients. Brain. 2009; 132:671–683. [PubMed: 19190042]

Tranel D. Impaired naming of unique landmarks is associated with left temporal polar damage. Neuropsychology. 2006; 20:1–10. [PubMed: 16460217]

Turken AU, Dronkers NF. The neural architecture of the language comprehension network: Converging evidence from lesion and connectivity analyses. Frontiers in Systems Neuroscience. 2011; 5:1. [PubMed: 21347218]

Ueno T, Saito S, Rogers TT, Lambon Ralph MA. Lichtheim 2: Synthesizing aphasia and the neural basis of language in a neurocomputational model of the dual dorsal-ventral language pathways. Neuron. 2011; 72:385–396. [PubMed: 22017995]

Van Dijk KR, Hedden T, Venkataraman A, Evans KC, Lazar SW, Buckner RL. Intrinsic functional connectivity as a tool for human connectomics: Theory, properties, and optimization. Journal of Neurophysiology. 2010; 103:297–321. [PubMed: 19889849]

Visser M, Jefferies E, Lambon Ralph MA. Semantic processing in the anterior temporal lobes: A meta-analysis of the functional neuroimaging literature. Journal of Cognitive Neuroscience. 2010; 22:1083–1094. [PubMed: 19583477]

Visser M, Lambon Ralph MA. Differential contributions of bilateral ventral anterior temporal lobe and left anterior superior temporal gyrus to semantic processes. Journal of Cognitive Neuroscience. 2011; 23:3121–3131. [PubMed: 21391767]

Waldron EJ, Manzel K, Tranel D. The left temporal pole is a heteromodal hub for retrieving proper names. Frontiers in Bioscience (Schol Ed). 2014; 6:50–57.

Warren JE, Crinion JT, Lambon Ralph MA, Wise RJ. Anterior temporal lobe connectivity correlates with functional outcome after aphasic stroke. Brain. 2009; 132:3428–3442. [PubMed: 19903736]

Warrington EK, Shallice T. Category specific semantic impairments. Brain. 1984; 107:829–854. [PubMed: 6206910]

Whitney C, Kirk M, O'Sullivan J, Lambon Ralph MA, Jefferies E. Executive semantic processing is underpinned by a large-scale neural network: Revealing the contribution of left prefrontal, posterior temporal, and parietal cortex to controlled retrieval and selection using TMS. Journal of Cognitive Neuroscience. 2012; 24:133–147. [PubMed: 21861680]

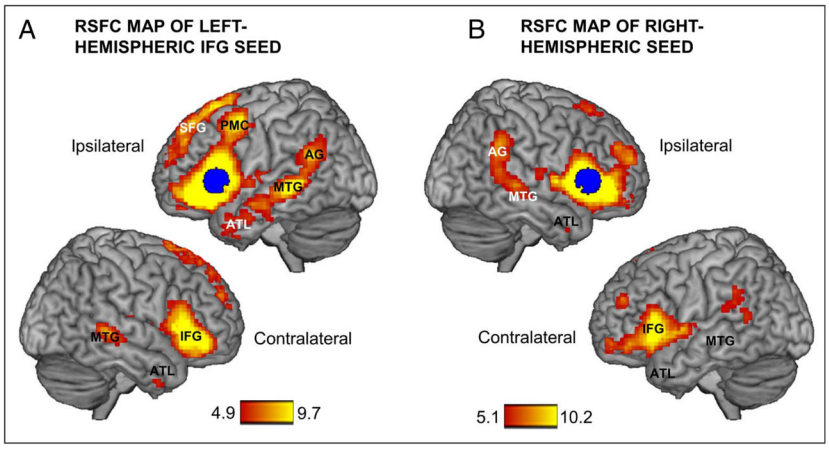

Figure 1.

RSFC of the IFG seeds. *t* Maps show voxels (in yellow–red) where spontaneous hemodynamic activity is significantly correlated (FDR $p < .001$) with activity in the seed region (in blue). (A) Left IFG, considered to be at the core of "Broca's area," shows ipsilateral connectivity with ATL. (B) Right IFG is not connected with either the left or right ATL. AG = angular gyrus; PMC = premotor cortex; SFG = superior frontal gyrus.

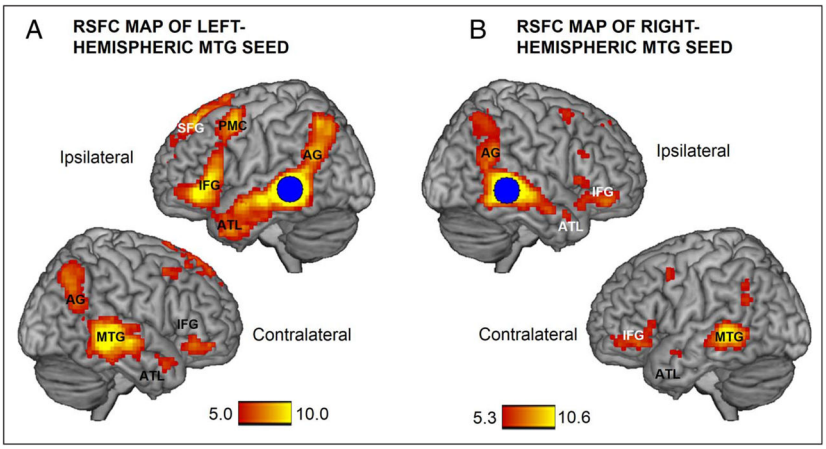

Figure 2.

RSFC of MTG seeds. (A) The left MTG shows extensive ipsilateral connections with ATL and with frontal structures including IFG, PMC, and SFG. (B) Right MTG shows relatively sparse ipsilateral and contralateral connectivity with ATL and with frontal structures. FDR $p < .001$.

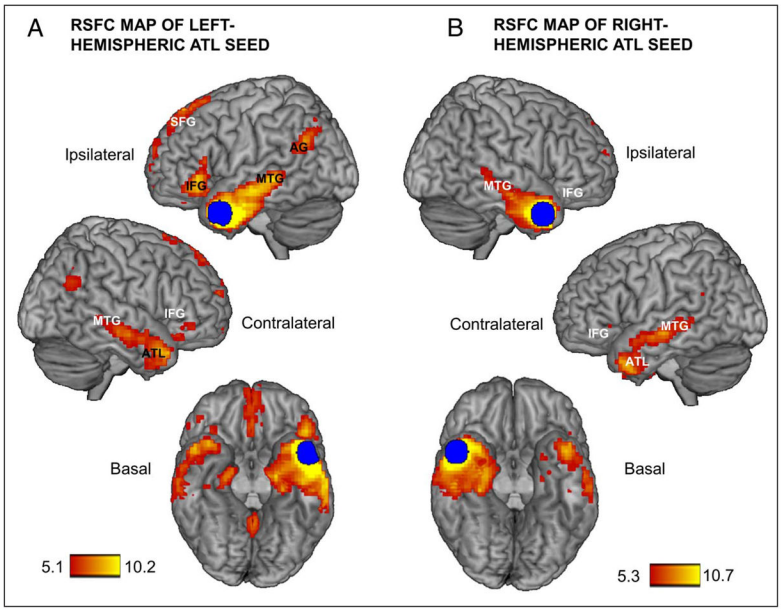

Figure 3.

RSFC of seeds in lateral ATL. (A) Left ATL shows long-range ipsilateral connections with IFG, AG, and SFG. (B) Right ATL fails to show these connections, either ipsilaterally or contralaterally. FDR $p < .001$.

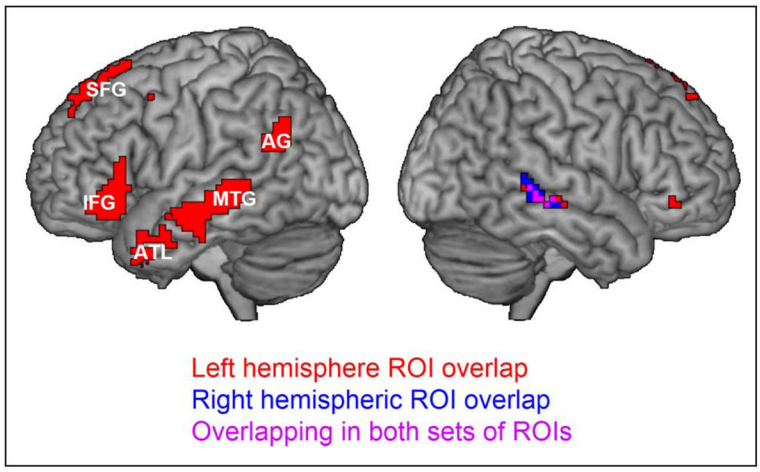

Figure 4.

Overlap of RSFC maps from left- and right-hemispheric ROIs. IFG, MTG, and ATL in the left hemisphere share common connections with a network of ipsilateral structures (in red), including interconnections around each seed area plus long-range connections with parietal (SFG) and frontal (AG) regions. In contrast, there was very little overlap between three homotopic ROIs in the right hemisphere (in blue–purple).

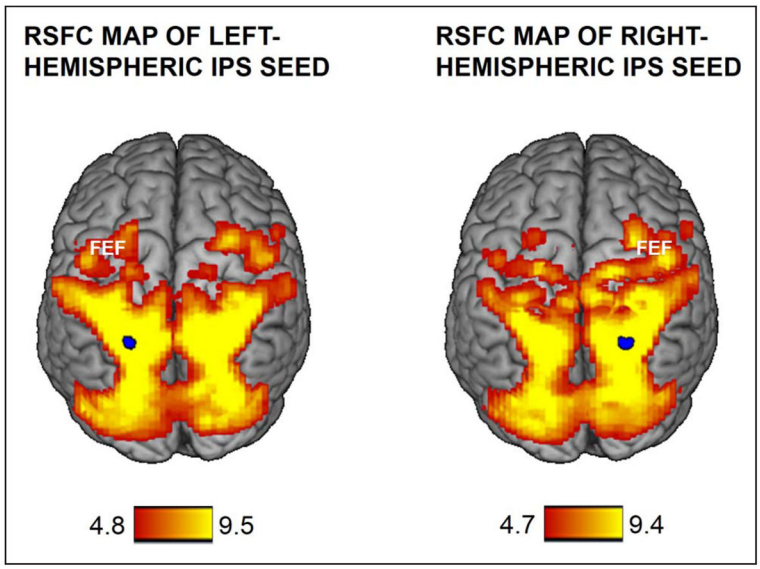

Figure 5.

RSFC of spatial attention seeds. RSFC maps from left-hemispheric and right-hemispheric seeds in the intraparietal sulci (IPS) are largely symmetrical, both showing ipsilateral and contralateral connections with frontoparietal structures including the FEFs. FDR $p < .001$.

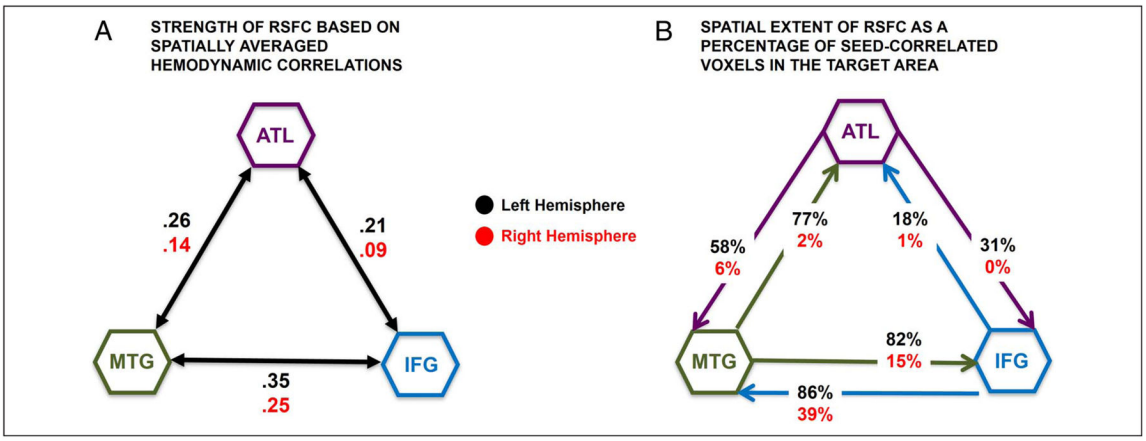

Figure 6.

Strength and spatial extent of functional connectivity between ROIs. Two complementary methods were used to quantify the degree to which hemodynamic activity in ipsilateral ROIs was intercorrelated. Left hemispheric correlations and voxel counts are shown in black, right hemispheric in red. (A) Correlations between the voxel-averaged hemodynamic time series from each ROI. All correlations are stronger in the left hemisphere compared with the right hemisphere. (B) Percentage of gray matter voxels in each target region where activity was significantly correlated with the seed region (FDR $p < .001$). Arrows extend from seed regions to target regions. All targets contained more correlated voxels in the left hemisphere.

Table 1

Correlations between ROI Time Series

ROI Pairs	Hemispheric Comparison	Correlation z(r) ± SD	t	df	p
IFG–ATL	Left (one-sample)	.21 ± .22	5.4	32	<.001
	Right (one-sample)	.09 ± .17	3.1	32	.004
	Left vs. right (paired)	–	2.8	32	.008
IFG–MTG	Left (one-sample)	.35 ± .18	11.3	32	<.001
	Right (one-sample)	.25 ± .23	6.1	32	<.001
	Left vs. right (paired)	–	2.9	32	.007
ATL–MTG	left (one-sample)	.26 ± .19	7.9	32	<.001
	right (one-sample)	.14 ± .18	4.2	32	<.001
	left vs right (paired)	–	3.2	32	.003
IPS–FEF	left (one-sample)	.31 ± .22	7.9	32	<.001
	right (one-sample)	.30 ± .19	9.2	32	<.001
	left vs right (paired)	–	0.1	32	.90

The *Z*-transformed Pearson correlations between activity in each possible pair of ipsilateral language ROIs (IFG, MTG, and ATL) are listed. These correlation coefficients are also schematized in Figure 4A. One-sample *t* tests show that all correlations significantly differed from zero. Left hemispheric correlation coefficients were then compared with their counterparts in the right hemisphere via paired-samples *t* tests. All tests were significant, showing that left hemispheric correlations are of significantly higher magnitude. In contrast, activity in spatial attention nodes (IPS and FEF) was correlated to a similar degree in both hemispheres.